

Local Structure of Amorphous Organotin Sulfide Clusters by Low-Energy X-Ray Absorption Fine Structure

Jens R. Stellhorn,* Shinjiro Hayakawa, Benjamin D. Klee, Benedict Paulus, Jonathan Link Vasco, Niklas Rinn, Irán Rojas León, Stefanie Dehnen, and Wolf-Christian Pilgrim

The local structure of four amorphous organotin sulfide compounds exhibiting nonlinear optical (NLO) properties is investigated by low-energy X-ray absorption spectroscopy (XANES and EXAFS). The basic structural motif of a heteroadamantane cluster with different organic substituents is confirmed by the experiments and by comparison with computer simulations of the near-edge structure. Essential information is obtained on a special role of the nonaromatic but electron-rich cyclopentadienyl substituents, which are able to affect the structure of the heteroadamantane cluster core. The EXAFS fits also indicate a structural distinction between two groups within these compounds, which exhibit fundamentally different NLO responses: compounds that show a second harmonic generation can be described well using the single-molecule approach, whereas the compounds exhibiting the generation of a supercontinuum manifest additional structural contributions.

1. Introduction

Compounds of the general composition $[(R\text{Sn})_4\text{S}_6]$ (R = organic substituent) were recently found to exhibit strong nonlinear optical (NLO) effects. Depending on their morphology and the type

of organic substituent, they can potentially be used as cheap and efficient warm-white light emitters when driven by a low-power continuous-wave infrared laser diode.^[1–3] This so-called white-light generation (WLG) is the common denomination of a physical phenomenon referred to as supercontinuum generation, i.e., the extreme spectral broadening of a light source propagating through a nonlinear medium.^[4,5] WLG was demonstrated for amorphous $[(R\text{Sn})_4\text{S}_6]$ compounds with electron-rich organic substituents, like phenyl (Ph), cyclopentadienyl (Cp), or benzyl (Bn).^[6] On the other hand, a variation of the organic substituent can change the NLO response, leading instead to a strong second harmonic generation (SHG) in amorphous compounds with R = methyl (Me) or naphthyl (Np).^[2]

Density functional theory (DFT) calculations suggest that these compounds consist of $\{\text{Sn}_4\text{S}_6\}$ cluster cores in a heteroadamantane configuration, with the organic substituents chemically bound to Sn.^[2,6] An illustration of the cluster geometries is shown in **Figure 1**. The most recent DFT study^[7] also indicates that the relative orientation of neighboring clusters significantly affects the strength and the nature of the NLO effect.

In principle, the structure of the $\{\text{Sn}_4\text{S}_6\}$ cluster core has a closely related isomer, which has a “double-decker”-type configuration. This structure was expected to be the less likely isomer, based on an energy difference of the DFT models of about 28 kJ mol^{-1} and for practical considerations (the adamantane type does not possess inversion symmetry, which is regarded as an requirement for the NLO properties). However, due to the amorphous and molecular nature of this material, an experimental proof for any specific structure is difficult to obtain. First, experimental proofs were only recently obtained from X-ray scattering experiments coupled with reverse Monte Carlo modeling,^[8,9] which provides a means to fit the experimental data with a 3D ensemble of structural units (which here are the molecular clusters), for the case of the $[(\text{PhSn})_4\text{S}_6]$ cluster,^[10] favoring the adamantane-like molecular structure.

To gain an insight into the local structure of these compounds, we performed low-energy X-ray absorption spectroscopy measurements at the S K and Sn L_3 absorption edges. The near-edge structure contains information on the local electronic properties (in particular on the nonoccupied density of states) as well as on structural features (chemical bonds as well as long- or

J. R. Stellhorn, S. Hayakawa
Department of Applied Chemistry
Hiroshima University
Hiroshima 739-8527, Japan
E-mail: stellhoj@hiroshima-u.ac.jp

J. R. Stellhorn, B. D. Klee, B. Paulus, J. Link Vasco, N. Rinn, I. Rojas León,
S. Dehnen, W.-C. Pilgrim
Department of Chemistry
Philipps University Marburg
35032 Marburg, Germany

B. D. Klee
Institute for Solid State Physics and Optics
Wigner Research Centre for Physics
Budapest 1121, Hungary

 The ORCID identification number(s) for the author(s) of this article can be found under <https://doi.org/10.1002/pssb.202200088>.

© 2022 The Authors. physica status solidi (b) basic solid state physics published by Wiley-VCH GmbH. This is an open access article under the terms of the Creative Commons Attribution-NonCommercial License, which permits use, distribution and reproduction in any medium, provided the original work is properly cited and is not used for commercial purposes.

DOI: 10.1002/pssb.202200088

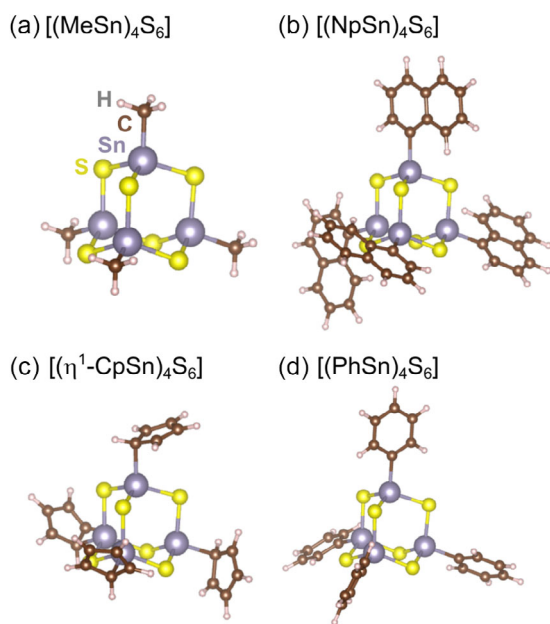


Figure 1. Models of the four clusters from DFT simulations.^[2,6]

intermediate-range interactions). The interpretation of an X-ray absorption near-edge structure (XANES) spectrum can be rather challenging, however, and is therefore effectively assisted by computer simulations.

With this approach, we aim to provide a decisive step forward to understand the yet puzzling physical mechanisms behind the different NLO effects in these systems.

2. Experimental Details and Data Analysis

We prepared four different samples of the general composition $[(R\text{Sn})_4\text{S}_6]$ with the organic substituents R being methyl (Me), naphthyl (Np), cyclopentadienyl (Cp), and phenyl (Ph). The samples were prepared by reaction of $R\text{-SnCl}_3$ with Na_2S in toluene. More details of the sample preparation are given elsewhere.^[1,6]

The S K extended X-ray absorption fine structure (EXAFS) (2.47 keV) and the Sn L_3 XANES (3.93 keV) spectroscopy experiments were conducted at BL11 of the Hiroshima Synchrotron Radiation Center (HSRC), Hiroshima University, Higashi-Hiroshima, Japan. This beamline is designed to maximize the beam intensity on the sample in the 2–5 keV region by forgoing the use of Be windows (the beamline shares the vacuum directly with the storage ring) and minimizing air paths.^[11] The synchrotron radiation from a bending magnet was monochromatized with a Si(111) double-crystal monochromator. A Ni-coated pre-mirror system is utilized to effectively reject higher harmonics. To detect the incident flux, a commercial ionization chamber filled with an N_2/He (20:80) mixture was placed between the end of the beamline and the sample chamber. The beam size at the sample position is approximately $3\text{ mm} \times 1\text{ mm}$. The sample chamber was filled with He to reduce air absorption. The transmitted beam is detected by another ionization chamber filled with air, while the fluorescence intensity was measured with a Si drift detector (SDD). For the sample preparation, a fine

layer of the sample (about 1–2 mg in an area of 1 cm^2 , corresponding to about 1.5 absorption lengths) was placed between two thin polypropylene films ($6\text{ }\mu\text{m}$ thickness), and was oriented with a 45° angle to the beam, to allow for the simultaneous measurement of transmission (S K XANES and EXAFS) and fluorescence intensity (Sn L_3 XANES).

The EXAFS data were analyzed with the DEMETER program package.^[12] For modeling the S K EXAFS data, initial models for the respective cluster from DFT simulations^[2,6] were used. The models are illustrated in Figure 1. The S–Sn and S–S distances and mean displacements were used as fitting parameters. The latter exhibit comparably large uncertainties due to the low-energy region and the limited accessible k -range and were therefore constrained between 0.008 and 0.018 \AA^2 .

For comparison, we calculated XANES spectra using the single molecule reference structures. The simulations were performed using the FDMNES software.^[13] This software uses the atomic positions of a given cluster and calculates the absorption cross sections around every atom in a given radius. In our simulations, the radius was set to 9 \AA , comprising almost the entire molecule. The calculations are based on the finite difference method (FDM) to solve the Schrödinger equation.^[13] The XANES spectra of every S (or Sn, respectively) atom are summed up and convoluted in order to simulate the broadening due to the finite core-hole lifetime. Furthermore, the simulations also allow for the calculation of crystal orbital overlap populations (COOP), which can reveal additional information on the chemical bonds, including bonding and antibonding interactions.^[14]

3. Results

The XANES data provide an initial view of the atomic-scale structural arrangements. They are displayed in Figure 2 (S K edge) and Figure 3 (Sn L_3 edge) for all four compounds. The figures

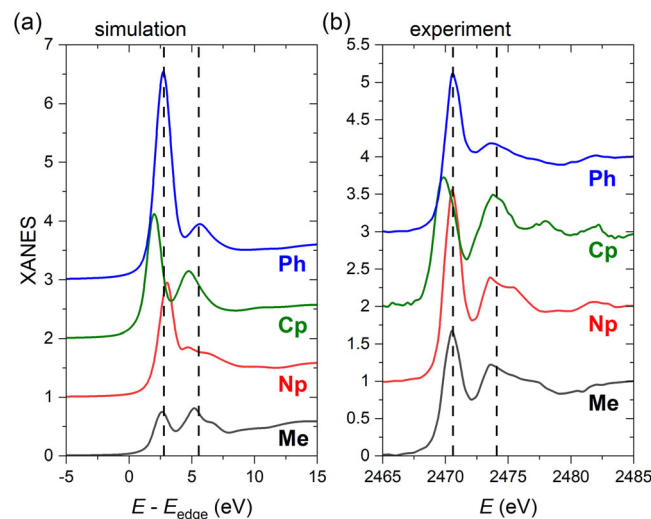


Figure 2. XANES data for the four organotin sulfide samples (Me: black, Np: red, Cp: green, Ph: blue, shifted upward for clarity) at the S K edge. a) FDMNES simulations in comparison with b) experimental data. The vertical dashed lines are guides for the eye, indicating the position of the main peaks.

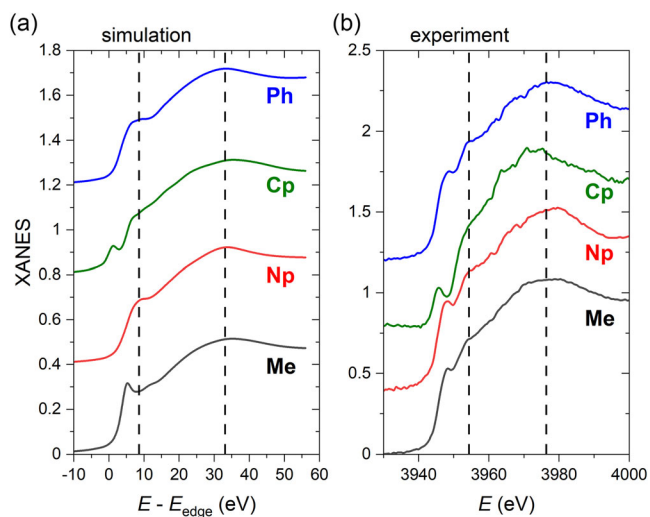


Figure 3. XANES data for the four organotin sulfide samples (Me: black, Np: red, Cp: green, Ph: blue, shifted upward for clarity) at the Sn L_3 edge. a) FDMNES simulations in comparison with b) experimental data. The vertical dashed lines are guides for the eye, indicating the position of the main peaks.

also provide a comparison with the FDM simulations. The experimental data in general exhibit a two-signal structure at the S K edge (marked with the vertical dashed lines) and a preedge shoulder before the main peak at the Sn L_3 edge (also marked as vertical dashed lines). It is readily observed that the cluster with Cp substituents differs significantly from the others: the maxima of the XANES signals of both S K and Sn L_3 are shifted to lower

energies (by 0.8 and 3.5 eV, respectively); furthermore, the structure of the signal is also considerably different from the other samples, with the two main signals of the S K XANES at nearly equal height (the other samples exhibit considerably larger first peaks at about 2470.6 eV) and with a shifted and more distinct preedge peak in the Sn L_3 XANES.

The FDM simulations show a generally good agreement with the experimental data, reproducing the general form of the signal for all clusters in both S K and Sn L_3 XANES curves, and also reproducing the shift of the signal of the $[(\text{CpSn})_4\text{S}_6]$ cluster at the S K edge (shift by 0.73 eV). However, the simulations fail to reflect the relative intensities of the signals at the S K edge (in particular for the $[(\text{PhSn})_4\text{S}_6]$ cluster, where the first peak is considerably diminished in the experimental data), and also do not reproduce the shift of the main peak of the $[(\text{CpSn})_4\text{S}_6]$ cluster at the Sn L_3 edge. Overall, it is still a remarkably good agreement considering that the reference values are determined for an isolated molecule, whereas the experimental data represent the situation of the structure in the amorphous phase, in which the clusters are packed relatively tightly.^[10,15] The differences between the simulations and the experiment are presumably related to additional distortions of the clusters and/or intermolecular interactions.

The S K EXAFS data and the best fit results are illustrated for all four systems in k -space and in real space in **Figure 4a,b**, respectively. It is found that the EXAFS data in general can be fitted reasonably well for the clusters with R = Me and Np, but not so well for R = Cp and Ph. The fit results for the interatomic distances are illustrated in **Figure 5**, along with the reference values from the DFT simulations.

The S—Sn bond length agrees with the reference values within the experimental errors; only the cluster with Cp substituents

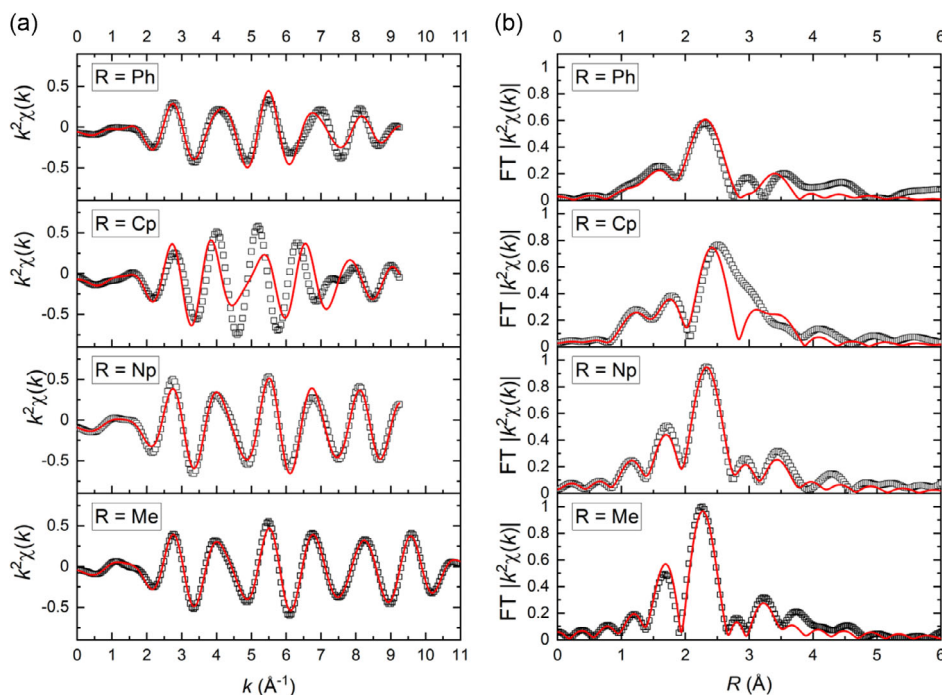


Figure 4. Experimental data (squares) for the four different compounds and fits using the DFT model systems (red lines) in a) k -space and b) R -space. The R -space data are displayed as Fourier transform magnitudes of the EXAFS functions with k^2 -weighting.

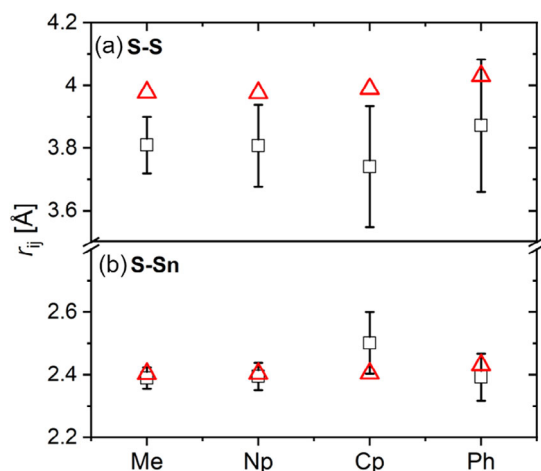


Figure 5. Fit results for the distances of the a) S–S and the b) S–Sn correlation. Experimental data (black squares, with error bars) in comparison with reference values from the DFT models (red triangles).

exhibits an elongated S–Sn bond—however, due to the “missing” part of the fit (the region between 2.5 and 3.0 Å in Figure 4b that is not well described by the fit), the error bar is quite large. The S–S correlations of this fitting approach are significantly shorter than the reference values for all clusters by about 0.2 Å, and have a considerable error bar. The error is in part due to the small accessible k -range, which renders the fitting of signals at larger distances more difficult.

The fitting qualities in particular for the clusters with $R = \text{Ph}$ and Cp could be improved by considering additional paths for the EXAFS fits. However, when including an additional S–S or S–Sn path at an intermediate distance, the fitting parameters show a considerable interdependence. At this stage, therefore, the inclusion of additional constraints or datasets (e.g., Sn K edge EXAFS) is necessary to get reliable information of these additional paths.

4. Discussion

Due to the large contribution of multiple scattering in the XANES regime, details about the 3D structure between the absorbing atoms and its neighbors (such as bond angles relative orientations) are in principle coded into the data. Although these are challenging to analyze, we can nevertheless compare XANES simulations for different structures, if reference models are available. In this case, we can compare the XANES simulations of the two possible isomers of the $\{\text{Sn}_4\text{S}_6\}$ cluster core, i.e., an adamantane type (AD) or a “double-decker” type (DD). For the example of a cluster with $R = \text{Ph}$, the FDM results are illustrated in **Figure 6**. It is immediately seen that the DD isomer leads to a very different XANES signal, which does not agree well with the experimental data. Thus, the XANES data provide an unequivocal experimental evidence for the adamantane-type structure.

Overall, we find that a simple description of the experimental data for all samples based on the single, isolated molecules (in the heteroadamantane configuration, shown in Figure 1 is already quite successful, and can reproduce the general form

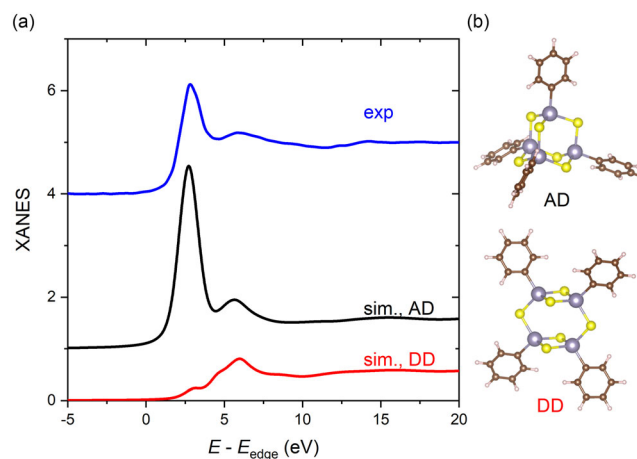


Figure 6. a) XANES simulation for the different isomers considered for the $[(\text{PhSn})_4\text{S}_6]$ cluster: the adamantane type (AD, black line) and double-decker type (DD, red line), in comparison with the experimental data (blue). The data are shifted upward for clarity. The respective cluster geometries are displayed in (b).

of the XANES signals (Figures 2 and 3) as well as the first peaks of the EXAFS data (S–Sn paths, Figures 4 and 5). This confirms that the basic structural motif, i.e., the heteroadamantane cluster core, is intact even in the amorphous phase.

The notable disparity from the DFT model concerning the S–S distances may indicate a certain flexibility of the S–Sn–S bond angle of the heteroadamantane cage for all compounds. For the clusters with Me and Np substituents (which exhibit satisfactory fit qualities), in a simplified view, the shortening of the average S–S distances by about 0.16 Å translates to a decrease of the S–Sn–S bond angle of about 6°. In principle, this should also lead to split peaks in the real space EXAFS data shown in Figure 4b, i.e., an additional peak at a correspondingly larger distance. While there are indeed observable signals in this range in Figure 4b, their assignment is not unambiguous due to the intensity decrease with R and the considerable effect of multiple scattering contributions in the range beyond 4 Å. These problems notwithstanding, we interpret the apparent distortions as an effect of the cluster–cluster interactions related to the dense packing of molecules in the amorphous phase.

The situation is even more complex in the clusters with Cp and Ph substituents, which do not show good fitting qualities in this second-neighbor distance range. This indicates that an adequate structural description of these two compounds needs additional correlations, possibly intermolecular interactions. The reasons may be found in the dispersive interactions of the π -electron systems: the recent DFT simulations,^[7] which compares cluster dimers for $R = \text{Ph}$ and Np, indicate much stronger interactions between the extended π systems of the Np substituents in contrast to the Ph substituents. In turn, these interactions have a considerable influence on the closest possible distance of the clusters. Therefore, it stands to reason that the intermolecular interactions are different for the two groups of compounds (i.e., Me- and Np- vs Cp- and Ph-substituted clusters). It is interesting that this apparent distinction corresponds to the change of the NLO response, i.e., the SHG that is observed

for R = Me and Np, while clusters with R = Cp and Ph exhibit WLГ. As already outlined above, however, in order to obtain reliable information on these additional paths, complementary experimental data are necessary (such as Sn K edge EXAFS).

Another important aspect is the shift of the XANES signal of the [(CpSn)₄S₆] to lower energies in the S K XANES data (Figure 2). From an analysis of the crystal orbital overlap population (COOP) available through the FDMNES simulations,^[14] we find that the main orbitals involved in the principal XANES peak are the σ^* orbitals formed by the contributions of the (S p_z -Sn s) and the (S p_z -Sn p_z) orbitals (note that the z direction is chosen along the interatomic axes). The σ^* orbitals are apparently destabilized by the additional electron density at the Sn atom, related to the electron-rich, but nonaromatic, Cp substituent, which transfers electron density into the cluster core. This destabilization appears to be supportive of the WLГ effect, e.g., in comparison with the clusters with Np substituents, but is not a strict requirement (since Ph-substituted clusters exhibit a similar NLO response).

As an outlook, we plan to extend the current investigations by measurements of the Sn K edge, which should be available in a large k-range, providing an improved R-space resolution in addition to the local environments around the Sn atoms.

5. Conclusion

We performed low-energy XANES and EXAFS experiments of four amorphous organotin sulfide compounds with R = Me, Np, Cp, and Ph. The XANES spectra are compared with simulations using the finite difference method, and the EXAFS data are fitted based on model systems obtained by DFT simulations. A basic structural motif of heteroadamantane clusters can be confirmed for all samples by the good agreement between experimental data and the XANES simulations, as well as from the EXAFS fits.

Concerning the [(CpSn)₄S₆] cluster, our investigations are able to explain the energetic shift of the XANES signal by a destabilization of the S-Sn σ^* orbitals, which are related to the electron-rich but nonaromatic substituents. The EXAFS data of the clusters with R = Me and Np can be fitted well with a model assuming only a single [(RSn)₄S₆] molecule, whereas the fits are more complex for clusters with Ph and Cp substituents. These difficulties are presumably related to distortions of the cluster core and/or intermolecular interactions. This hypothesis will be tested in a subsequent study including information on the local environment around Sn. If confirmed, the investigations of the local structure can provide valuable information on the physical origin of the NLO properties of these systems.

Acknowledgements

This work was supported by a Grant-in-Aid for Early-Career Scientists (grant no. 20K15027) from the Japan Society for the Promotion of Science (JSPS). The authors also express their gratitude for funding by the German Research Foundation (Deutsche Forschungsgemeinschaft, DFG), grant no. 398143140, related to the Research Unit FOR 2824

"Amorphous Molecular Materials with Extreme Non-Linear Optical Properties." The S K- and Sn L₃-edge experiments were performed at the beamline BL-11 in the HiSOR facility with the approval of the Hiroshima Synchrotron Radiation Center, Hiroshima University (proposal nos. 20AG034, 21AU003, and 21AG045).

Open Access funding enabled and organized by Projekt DEAL.

Conflict of Interest

The authors declare no conflict of interest.

Data Availability Statement

The data that support the findings of this study are available from the corresponding author upon reasonable request.

Keywords

amorphous compounds, extended X-ray absorption fine structure (EXAFS), local structure, nonlinear optical properties, X-ray absorption near-edge structure (XANES)

Received: February 28, 2022

Revised: March 18, 2022

Published online: April 15, 2022

- [1] N. W. Rosemann, J. P. Eussner, A. Beyer, S. W. Koch, K. Volz, S. Dehnen, S. Chatterjee, *Science* **2016**, 352, 6291.
- [2] N. W. Rosemann, J. P. Eussner, E. Dornsiepen, S. Chatterjee, S. Dehnen, *J. Am. Chem. Soc.* **2016**, 138, 16224.
- [3] S. Dehnen, P. R. Schreiner, S. Chatterjee, K. Volz, N. W. Rosemann, W.-C. Pilgrim, D. Mollenhauer, S. Sanna, *ChemPhotoChem* **2021**, 5, 1033.
- [4] R. R. Alfano, *The Supercontinuum Laser Source*, Springer, New York **2016**.
- [5] J. M. Dudley, G. Genty, S. Coen, *Rev. Mod. Phys.* **2006**, 78, 1135.
- [6] E. Dornsiepen, F. Dobener, S. Chatterjee, S. Dehnen, *Angew. Chem., Int. Ed.* **2019**, 58, 17041.
- [7] K. Hanau, S. Schwan, M. R. Schäfer, M. J. Müller, C. Dues, N. Rinn, S. Sanna, S. Chatterjee, D. Mollenhauer, S. Dehnen, *Angew. Chem., Int. Ed.* **2021**, 60, 1176.
- [8] R. L. McGreevy, L. Pusztai, *Mol. Simul.* **1988**, 1, 359.
- [9] O. Gereben, L. Pusztai, *J. Comput. Chem.* **2012**, 33, 2285.
- [10] B. D. Klee, E. Dornsiepen, J. R. Stellhorn, B. Paulus, S. Hosokawa, S. Dehnen, W.-C. Pilgrim, *Phys. Status Solidi B* **2018**, 255, 1800083.
- [11] S. Hayakawa, Y. Hajima, S. Qiao, H. Namatame, T. Hirokawa, *Anal. Sci.* **2008**, 24, 835.
- [12] B. Ravel, M. Newville, *J. Synchrotron Radiat.* **2005**, 12, 537.
- [13] a) O. Bunău, A. Y. Ramos, Y. Joly, in *International Tables for Crystallography*, International Union of Crystallography **2020**, <https://doi.org/10.1107/s1574870720003304>. b) O. Bunău, Y. Joly, *J. Phys.: Condens. Matter* **2009**, 21, 345501.
- [14] M. Diaz-Lopez, S. A. Guda, Y. Joly, *J. Phys. Chem. A* **2020**, 124, 6111.
- [15] B. D. Klee, B. Paulus, S. Hosokawa, M. T. Wharmby, E. Dornsiepen, S. Dehnen, W.-C. Pilgrim, *J. Phys. Commun.* **2020**, 4, 035004.